Acidic pH Promotes Dimerization of Bcl-2 Family Proteins

Zhihua Xie, Sharon Schendel, Shigemi Matsuyama, and John C. Reed*

The Burnham Institute, Program of Apoptosis & Cell Death Research, 10901 N. Torrey Pines Rd., La Jolla, California 92037

Received December 12, 1997; Revised Manuscript Received March 9, 1998

ABSTRACT: Several members of the apoptosis-regulating Bcl-2 family of proteins can homo- or heterodimerize with each other at neutral pH and can also form ion channels in synthetic membranes at low pH. The effects of low pH on dimerization among these proteins, however, have not heretofore been examined. Surface plasmon resonance was used to examine the kinetics of dimerization as a function of pH between the anti-apoptotic protein Bcl-X_L (applied in the mobile phase) and three other members of the Bcl-2 family: Bcl-2, Bax, and Bid (immobilized on biosensor chips). In all cases, the relative affinity of dimerization was substantially increased at pH 4.0 compared to pH 7.0−7.4, ranging from a ∼10-fold enhancement for Bcl-X_L/Bcl-X_L homodimers to >60-fold for Bcl-X_L/Bid heterodimers. Comparison of the apparent association (k_a) and dissociation (k_d) rates at neutral and acidic pH revealed that the major contributor to increased affinity at low pH was a decreased rate of dimer dissociation. Thus, low pH stabilizes homo- and heterodimeric complexes comprised of Bcl-X_L and these other Bcl-2 family proteins. At pH 4.0, the circular dichroism spectra of Bcl-X_L and Bax were essentially unchanged relative to pH 7.0−7.4, indicating a complete retention of α-helical secondary structure at low pH and excluding gross denaturation of the proteins. Size-exclusion chromatography and bisANS (4,4′-dianilino-1,1′-binaphthyl-5,5′-disulfonic acid) labeling studies provided indirect evidence that Bcl-X_L may undergo conformational changes at low pH. The findings are discussed with respect to the mechanisms of ion-channel formation by Bcl-2 family proteins and the putative molten globule state that has been proposed for these and structurally similar proteins.

Bcl-2 family proteins are important regulators of programmed cell death and apoptosis (*1*−*3*). These proteins either inhibit or induce cell death, with the ratios of anti-apoptotic relative to pro-apoptotic members of the Bcl-2 family representing a critical determinant of the ultimate sensitivity or resistance of mammalian cells to various apoptotic stimuli. Many Bcl-2 family proteins can physically interact with themselves and each other, forming homo- and heterodimers (*1, 2*). In some instances, these dimerization events appear to play important roles in the regulation or effector functions of these proteins (*4*−*6*). Thus, a need exists to understand more about how dimerization among the Bcl-2 family proteins is controlled.

The domains within Bcl-2 and its homologues that are required for dimerization have been determined by deletional and mutational analysis, and these results were recently corroborated by X-ray crystallographic and NMR-based structural studies (*4, 5, 7*−*15*). The 3-dimensional structure of the Bcl-X_L protein consists of seven α-helices joined by flexible loops of variable length (*14*). Amino acid sequence alignments of Bcl-2 family proteins have demonstrated up to four evolutionarily conserved domains, termed Bcl-2 homology (BH) domains: BH1, BH2, BH3, and BH4. The BH4 and BH3 domains correspond to the first and second amphipathic α-helices in these proteins, as predicted from the 3-dimensional structure of Bcl-X_L (*14*). The BH1 domain begins within a loop located upstream of the fifth α-helix in Bcl-X_L and extends partially into this α-helix. The BH2 domain corresponds to the latter portion of the sixth α-helix and loop which follows.

The BH1, BH2, and BH3 domains in combination form the borders of a hydrophobic pocket located on the surface of the Bcl-X_L protein. Mutation of particular residues lining this pocket has been shown to abolish dimerization (*7, 12*). Thus, this surface pocket appears to function analogous to a receptor, binding regions located on partner proteins that dimerize with Bcl-2 and Bcl-X_L. In contrast, the BH3 domain by itself is sufficient to insert into the surface pocket created by the combination of BH1, BH2, and BH3, perhaps serving as a peptide-ligand that mediates dimerization among Bcl-2 family proteins (*5, 11, 13, 15*−*18*). This finding implies that at least some Bcl-2 family proteins could exist in two states: one in which the protein creates a receptor-like pocket and the other in which the amphipathic α-helix that comprises BH3 rotates outward to expose its hydrophobic surface which then buries into the receptor-like pocket on dimerization partner proteins (*15*).

Some pro-apoptotic members of the Bcl-2 family, including Bid, Hrk, and Bik, contain only a BH3 domain (*4, 5, 13*). Deletion of the BH3 domains from these proteins uniformly abolishes dimerization with other members of the family and nullifies their function as inducers of cell death. Thus, the BH3 domain is apparently sufficient to modulate the functions of anti-apoptotic Bcl-2 proteins such as Bcl-2

† This work was supported by CaP-CURE and the California Breast Cancer Research Program (1RB-0093).

* Address correspondence at 619-646-3140 (phone), 619-646-3194 (fax), jreed@burnham-institute.org (e-mail).

S0006-2960(97)03052-3 CCC: $15.00 © 1998 American Chemical Society
Published on Web 04/15/1998

and Bcl-X_L. It has not been determined whether these "BH3-only" members of the Bcl-2 family must undergo conformational changes to expose the hydrophobic face of their BH3 domains for insertion into the pockets on Bcl-2 and Bcl-X_L.

An intriguing characteristic of many Bcl-2 family proteins is their predicted structural similarity to the pore-forming domains of bacterial toxins such as diphtheria toxin (DT) and the colicins (*14*). Though the 3-dimensional structure has been determined thus far only for Bcl-X_L, both anti-apoptotic proteins such as Bcl-2 and pro-apoptotic proteins such as Bax can be modeled easily on the same crystallographic coordinates, suggesting they share overall structural similarity (*19*). Consistent with these ideas, recombinant Bcl-2, Bcl-X_L, and Bax proteins have been shown to form ion-conducting channels in vitro in both liposomes and planar bilayers (*20*−*23*). In contrast, most of the BH3-only subgroup of Bcl-2 family proteins do not appear to share the same fold with Bcl-X_L, implying that they lack pore-forming capability (unpublished observations).

By analogy to the bacterial toxins, it has been speculated that the process of pore formation by Bcl-2 family proteins involves the membrane insertion of two α-helices normally buried in the interior of the compact folded protein. Indeed, deletion of these two hydrophobic core α-helices (α5 and α6) abolishes channel formation by Bcl-2 in vitro and destroys its ability to block cell death induced by Bax in mammalian cells and yeast (*21*). The process of channel formation in vitro by Bcl-2 family protein and the pore-forming domains of their structurally related bacterial toxins is highly pH dependent, with optima typically of pH ∼4.0 (*20*−*23*). Thus, acidic pH has been speculated to facilitate a conformational change in Bcl-2 family proteins which allows them to insert the putative pore-forming α5 and α6 helices perpendicularly into the lipid bilayer.

How the process of channel formation may be related to the ability of many Bcl-2 family proteins to homo- or heterodimerize remains unknown. The structure of Bcl-X_L reveals only two α-helices of sufficient length and hydrophobicity to span the lipid bilayer (α5 and α6). Consequently, it has been proposed that the minimum stoichiometry for a Bcl-X_L or Bcl-2 channel is a dimer of membrane-integrated proteins with each contributing a pair of α-helices to the channel (*21*). This reasoning derives from previous attempts to create channels in vitro using synthetic amphiphatic peptides, which revealed a four α-helix bundle as the minimum structure necessary to create an ion channel in vitro (*24*, *25*). Since in vitro channel formation in liposomes is dependent on low pH, it is important to understand how pH might influence dimerization among Bcl-2 family proteins.

In this report, we employed surface plasmon resonance (SPR)[1] (*26*−*30*) to characterize the kinetics of interactions of Bcl-X_L with several other members of the Bcl-2 family, including the anti-apoptotic protein Bcl-2, the pro-apoptotic protein Bax, and the pro-apoptotic BH3-only protein Bid. The findings suggest the existence of different conformational states which can markedly affect the dimerization properties of these proteins and show that acidic pH favors dimerization among these proteins primarily by slowing their rates of dissociation.

MATERIALS AND METHODS

Production and Purification of Recombinant Bcl-2 Family Proteins. The construction of most plasmids used for expression of Bcl-2 family proteins in bacteria has been described (*10*, *21*, *31*). For production of a mutant of Bcl-2 lacking the BH3 domain (Δ93−107), a two-step PCR approach was employed using pET-21a-Bcl-2 (ΔTM) (*21*) as the DNA template and two pairs of primers: (1) 5′-GCGGAATTCATGGCGCACGCTGGGAGAACA-3′ with 5′-CACAGGTGGCACCGGGCTGAGCGCAGG-3′; and (2) 5′-GTGCCACCTGTGTACCGCCGCGACTTCGCCGAGATG-3′ with 5′-CGCCTCGAGTCACTTCAGAGACAGCCAGGAGAAATC-3′. The two resulting PCR products were gel purified and mixed, and PCR was performed again using the outer primers, followed by digestion with *Eco*RI and *Xho*I. The resulting fragment was subcloned into pET-21a. All protein preparations were >95% pure, as determined by Coumassie staining of SDS−PAGE gels.

His_6-Tagged Proteins. His_6-human Bcl-2 (1−218), Bcl-2 (ΔBH3), and human Bcl-X_L (1−211) were expressed with an N-terminal His_6-tag using a modified pET vector (Novagen, Inc.) that removed the T7 protein 10 sequences (*32*), thus excluding any additional amino acids between the His_6 and first methionine of Bcl-2 and Bcl-X_L. Both proteins were expressed in BL21(DE3) cells. Briefly, a single colony was inoculated into 1 L of LB media containing 50 μg/mL ampicillin and grown at 37 °C overnight. The culture was then diluted by half with fresh LB/ampicillin and cooled to room temperature for an hour, before inducing with 1 mM IPTG for 6 h at ∼25 °C.

For purification of His_6−Bcl-2 and His_6−Bcl-2 (ΔBH3), cells from 1 L of culture were resuspended into 50 mL of 50 mM phosphate buffer (pH 6.8), 150 mM NaCl, and 1% (v/v) Tween 20 and then incubated with 0.5 mg/mL lysozyme at 25 °C for 0.5 h, followed by sonication to reduce viscosity. After centrifugation at 27500*g* for 10 min, the resulting pellets were washed twice with the same buffer and solubilized in 50 mM phosphate-buffered (pH 6.8) 6 M guanidinium-hydrochloride (GuHCl). Supernatants were collected and incubated with 10−20 mL of nickel resin (Qiagen, Inc.) at 4 °C for 3 h. The resin was washed with 50 mM phosphate-buffered (pH 6.8) 25 mM imidazole, 4 M GuHCl, and 0.1% Tween until the OD_{280} reached ≤0.01, followed by continued washing with 5 vol of 50 mM phosphate-buffered (pH 6.8) 25 mM imidazole and 4 M GuHCl. Proteins were eluted in 0.2 M acetic acid and 4 M GuHCl. Eluted His_6−Bcl-2 and His_6−Bcl-2 (ΔBH3) proteins were dialyzed against 25 mM acetic acid at 4 °C overnight, passed through 0.22 μm Whatmann filters and stored at −20 °C.

His_6−Bcl-X_L was purified under native conditions. Briefly, after sonication, the supernatant was incubated with 20 mL of nickel resin in 50 mM phosphate-buffered (pH 6.8) 150 mM NaCl, 1% Tween, and 25 mM imidazole at 4 °C for 3 h. The resin was washed with 50 mM phosphate-buffered (pH 6.8) 150 mM NaCl, 0.1% Tween, and 25 mM imidazole until the OD_{280} reached ≤0.01. His_6−Bcl-X_L was eluted with 250 mM imidazole in same buffer, followed by further purification by FPLC on a Mono Q (HR 10/10) column

[1] Abbreviations: RU, response units; TM, transmembrane; SPR, surface plasmon resonance.

(Pharmacia) using a linear gradient of 0.5 M NaCl at pH 8.0.

GST-Fusion Proteins. The GST-Bcl-X_L (1−211), GST-mouse Bax (1−171), and GST-mouse BID proteins were expressed in XL-1 Blue cells (Stratagene, Inc.) from the plasmids pGEX-4T-1 (*10, 31, 33*). Briefly, cells were grown in 2 L of LB with 50 μg/mL ampicillin at 37 °C to an OD_{600nm} of 1.0. IPTG (0.4 M) was then added, and cultures were incubated at 25 °C for 6 h. Cells were then recovered and incubated with 0.5 mg/mL lysozyme in 50 mM Tris (pH 8.0), 150 mM NaCl, 1% Tween, 0.1%, 2-mercaptoethanol, 5 mM EDTA, 1 mM PMSF, and a mixture of other protease inhibitors (Boehringer 1697498) at room temperature for 0.5 h, followed by sonication (*21*). Cellular debris was pelleted by centrifugation at 27500*g* for 10 min, and the resulting supernatants were incubated with 30 mL of glutathionine-Sepharose (Pharmacia) at 4 °C for 4 h. The resin was washed with 20 mM Tris (pH 8.0), 150 mM NaCl, 0.1% Tween, and 0.1% 2-mercaptoethanol until the OD_{280nm} reached ≤0.01. For removal of GST, the resin containing bound GST-fusion proteins was incubated with 10 units of thrombin (Boehringer, Inc.) at 4 °C in 20 mM Tris (pH 8.0), 150 mM NaCl, 0.1% 2-mercaptoethanol, 0.1% Tween 20, and 2.5 mM $CaCl_2$ overnight, and the released Bcl-X_L and Bax were then purified on Mono Q (HR 10/10) by FPLC using a linear gradient of 0.5 M NaCl at pH 8.0. BID was purified on Mono S (HR 10/10) using a linear gradient of 0.5 M NaCl at pH 5.0.

Gel-Filtration Chromatography. Purified protein samples (20−50 μg in 50 μL) were injected into a Superdex 200 column (HR 10/30) (Pharmacia) which had been equilibrated with various buffers as described in the text. Chromatography was performed using a flow rate of 0.8 mL/min by FPLC, monitoring absorbance at OD_{280nm}. A mixture of proteins that served as molecular weight markers (Bio-Rad) was used for column calibration.

Surface Plasmon Resonance. Kinetic measurements were performed using a BIAcore-II instrument with CM5 sensor chips and an Amine Coupling Kit (Pharmacia Biosensor AB, Sweden). For immobilization of proteins, the sensor chip was equilibrated with HB flow buffer [10 mM Hepes (pH 7.4), 150 mM NaCl, and 3.4 mM EDTA] at 5 μL/min, then activated by injecting 17 μL of 0.2 M *N*-ethyl-*N*′-(3-diethylaminopropyl)-carbodiimide and 0.05 M *N*-hydroxysuccinimide (NHS/EDC) followed by a 35 μL injection of Bcl-2 family or control proteins at 50−100 ug/mL in 10 mM acetate, pH 3.5−4.8. Excess NHS-esters on the surface were deactivated with 17 μL of 1 M ethanolamine-hydrochloride (pH 8.5). After immobilization, 10 μL of regeneration buffer [50 mM phosphate (pH 6.8) and 4 M GuHCl] was injected to remove noncovalently bound dimers.

For studying protein−protein interactions, kinetic data were obtained by diluting the samples in interaction buffer [HB buffer for neutral pH experiments, AB buffer consisting of 50 mM acetate (pH 4.0), 150 mM NaCl, and 3.4 mM EDTA, for low pH experiments] and injecting 20 μL at 10 μL/min across the prepared surface. The surface was regenerated after each injection with 5 μL of 50 mM phosphate (pH 6.8) and 4 M GuHCl. The rate constants k_{ass} and k_{diss} were calculated from the association and dissociation phases of the sensorgrams. The apparent affinity constants K_D were calculated directly from the kinetic parameters (k_{diss}/k_{ass}), while K_D(eq) was determined by Scatchard analysis, using the BIAcore software package (Pharmacia).

Peptides. A synthetic peptide corresponding to the BH3 domain of murine Bax (residues 57−72) with a Cys → Ser substitution (NH_2-KKLSESLKRIGDELDS-amide) or various control peptides were purchased from Chiron, Inc. and purified by C18 reverse phase HPLC to >90% purity.

BisANS Fluorescence. BisANS (4,4′-dianilino-1,1′-binaphthyl-5,5′-disulfonic acid) (Sigma, D4162) was diluted into 40 mM buffer (Tris-HCl, pH 8.0; Sodium phosphate, pH 7.0 or pH 6.0; Sodium acetate, pH 5.0, 4.0, or 3.0; or Gly-HCl, pH 2.5), 150 mM NaCl, and 3.4 mM EDTA to final concentration of 9.5 μM, without or with ∼0.2 μM Bcl-X_L. Samples were incubated at room temperature for 0.5 h. Fluorescence intensity was measured at 490 nm following excitation at 294 nm using a 5 nm slit width in a luminescence spectrometer (Perkin-Elmer LS50B). Recorded data were plotted against pH (*34*). Fluorescence intensities were corrected for buffer effects by subtraction of the appropriate blank.

Circular Dichroism. Circular dichroism measurements were carried out using a JASCO-J600 spectropolarimeter equipped with a temperature control accessory and calibrated with d_{10}-camphor sulfonate. Spectra were taken using cells of 1 mm path length, and recorded in 0.5 nm wavelength increments with a 2 s time constant and a full-scale sensitivity of 50 mdeg. Each spectrum is the average of four scans corrected for background solvent effects by subtraction of the appropriate blank. Bcl-X_L was dissolved in 20 mM DMG (dimethyl glutaric acid) and 150 mM NaCl, pH 4.0 or 7.0. To monitor changes in secondary structure, spectra were scanned in the far-UV from 200 to 250 nm. A value of 110 Da for the mean residue molecular weight was used in the calculation of the mean residue ellipticity, [Θ].

RESULTS

SPR Analysis of Bcl-2 Family Protein Interactions at Neutral pH. Using SPR, we evaluated the kinetics of interactions among recombinant purified His_6−Bcl-2, His_6−Bcl-X_L, Bax, and Bid. Most Bcl-2 family protein are anchored in intracellular membranes via a stretch of hydrophobic amino acids that constitutes a transmembrane (TM) domain (reviewed in ref *35*). For solubility purposes, these proteins were produced without their C-terminal ∼20 amino acids and purified to homogeneity (Figure 1).

Attempts to flow each of these proteins across dextran chips demonstrated that all but Bcl-X_L exhibited nonspecific interactions with the chip surface at low pH (data not shown). Therefore, Bcl-X_L was employed in the mobile phase for all SPR experiments, with Bcl-2, Bax, and Bid each immobilized on the chip surface. Bcl-X_L exhibited specific interactions with all Bcl-2 family proteins tested. Figure 2A, for example, shows typical sensorgrams obtained for interaction of immobilized Bcl-2 with various concentrations of Bcl-X_L in the mobile phase. When flowed over immobilized Bcl-2 chips in 150 mM NaCl solution at neutral pH, Bcl-X_L exhibited rapid binding until a steady-state equilibrium was reached, followed by rapid dissociation when the Bcl-X_L-containing mobile phase was replaced with flow buffer. The RU plateau obtained increased in a concentration-dependent

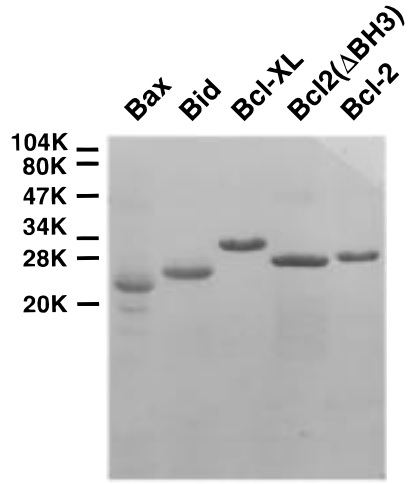

FIGURE 1: SDS−PAGE analysis of purified proteins. The purified human Bcl-2 (1−218), human Bcl-X_L (1−213), mouse Bax (1−171), and mouse Bid proteins were analyzed by SDS−PAGE (10 μg/lane in 12% gels) and stained with Coomassie. Molecular weight markers are indicated.

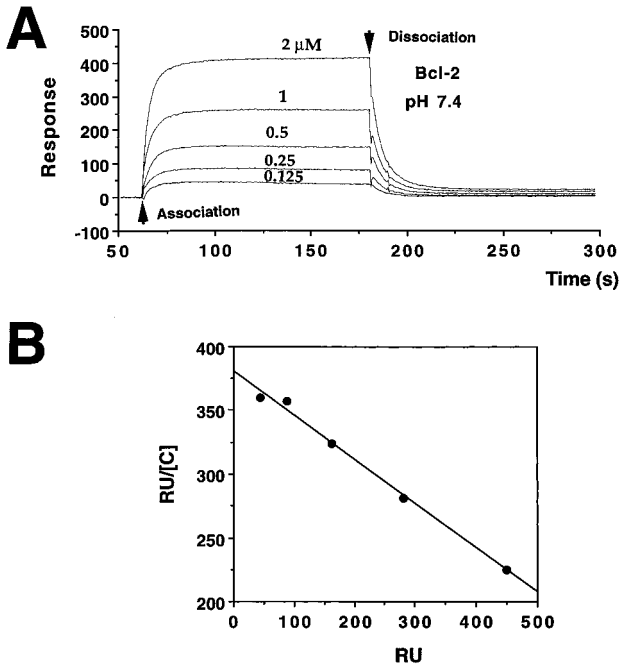

FIGURE 2: SPR analysis of Bcl-X_L interaction with Bcl-2. In panel A, typical sensorgrams are presented where various concentrations of Bcl-X_L (0.125, 0.25, 0.5, 1.0, and 2.0 μM, bottom to top) were flowed over a chip containing immobilized Bcl-2 protein (~5000 RU) at pH 7.4 in 150 mM NaCl and 3.4 mM EDTA. Bcl-X_L containing solution was applied at 10 μL/min. The binding and subsequent dissociation upon switching to flow buffer without Bcl-X_L were recorded. The chip was regenerated with 5 μL of 4 M GuHCl buffered with 50 mM sodium phosphate (pH 6.8). In panel B, a Scatchard plot of the equilibrium binding results is presented, using the plateau phase of the sensorgrams (RU) produced by flowing various concentrations [C] of Bcl-X_L over the Bcl-2-containing chip. The dissociation constant was estimated to be 2.8 μM ($1/K_a$) for this interaction.

manner. Essentially no binding of Bcl-X_L was detected by SPR when using dextran-control chips or certain mutants of Bcl-2 (see below).

Scatchard analysis of the data was performed by plotting RU/[C] versus RU for each concentration of Bcl-X_L used in the mobile phase (Figure 2B). A linear relationship between concentration and RU was observed for each of the immobilized Bcl-2 family proteins tested, including Bcl-2, Bax, and Bid, consistent with pseudo-first-order kinetic interactions. Figure 2B provides an example, showing the results obtained for Bcl-2/Bcl-X_L. The slopes of these plots were derived to obtain an apparent K_D for each protein−protein interaction at pH 7.4 in 150 mM NaCl (Table 1). On the basis of this analysis, the highest affinity interaction was obtained when using Bid in combination with Bcl-X_L, but all the apparent K_D values were within ~3-fold of each other (1.9−5.7 uM). Similar results were obtained using mobile-phase solutions containing nonionic detergents (0.1% Tween 20) and divalent cations (10 mM $MgCl_2$) (not shown). The rapid rate of dissociation made it difficult to accurately estimate K_D from kinetic data (k_d/k_a).

Table 1: Characteristics of Bcl-X_L Interactions with Bcl-2 Family Proteins

	K_D (μM)			kinetics (pH 4.0)		
	pH 7.4	pH 4.0	ΔK_D	k_a (μM^{-1} s^{-1})	k_d (s^{-1})	K_D (μM)
Bcl-XL/Bcl-2	2.8	0.16	18	0.32	0.05	0.16
Bcl-XL/Bax	4.6	0.11	42	0.34	0.04	0.12
Bcl-XL/Bid	1.9	0.03	63	0.32	0.009	0.03
Bcl-XL/Bcl-XL	5.7	0.42	14	0.27	0.12	0.44

Low pH Enhances Interactions among Bcl-2 Family Proteins. Under acidic conditions in vitro, the Bcl-2, Bcl-X_L, and Bax proteins can insert into lipid membranes, forming ion channels (*20*−*22*). Presumably, the dependence on low pH for this phenomenon reflects the need for a conformational change that allows the putative pore-forming fifth and sixth α-helices of these proteins to penetrate the lipid bilayer. To determine how low pH affects heterodimerization among Bcl-2 family proteins, we examined the kinetics and magnitude of binding of Bcl-X_L with immobilized Bcl-2, Bax, Bid, and Bcl-X_L by SPR over a range of pH values (2.5−8.0). The amount of Bcl-X_L interacting with chips containing immobilized Bcl-2 family proteins (as determined by RU) increased as the pH of the flow solution was lowered to pH 4.0, beyond which reduced interactions were observed. Figure 3A shows an example of sensorgrams obtained for the interaction of Bcl-X_L with immobilized Bcl-2 at various pHs, using fixed concentrations of Bcl-X_L in the flow solution and constant amounts of Bcl-2 on the chip. Maximum binding was obtained at pH 4.0 (Figure 3). The paucity of binding at neutral pH in this experiment can be attributed to the usage of 5-fold less Bcl-X_L compared to the previous experiments shown in Figure 2, where the binding was conducted at pH 7.4. The specificity of the enhanced interactions detected at lower pH between Bcl-X_L and immobilized Bcl-2 family proteins was confirmed by use of control proteins such as Bcl-2 (ΔBH3) in which the BH3 domain has been deleted, thus preventing its dimerization with other Bcl-2 family proteins (Figure 4).

Kinetic Analysis of Bcl-2 Family Interactions at Low pH Reveals a Slower Rate of Dissociation. The kinetics of Bcl-X_L binding to chips containing immobilized Bcl-2 family proteins were studied by SPR in experiments where various concentrations of Bcl-X_L were flowed over chips at pH 4.0. Figure 4 presents typical sensorgrams for chips coated with Bcl-2, Bax, Bid, and Bcl-X_L, as well as for control chips lacking an immobilized protein or containing Bcl-2 (ΔBH3) protein. In all cases, concentration-dependent binding of Bcl-

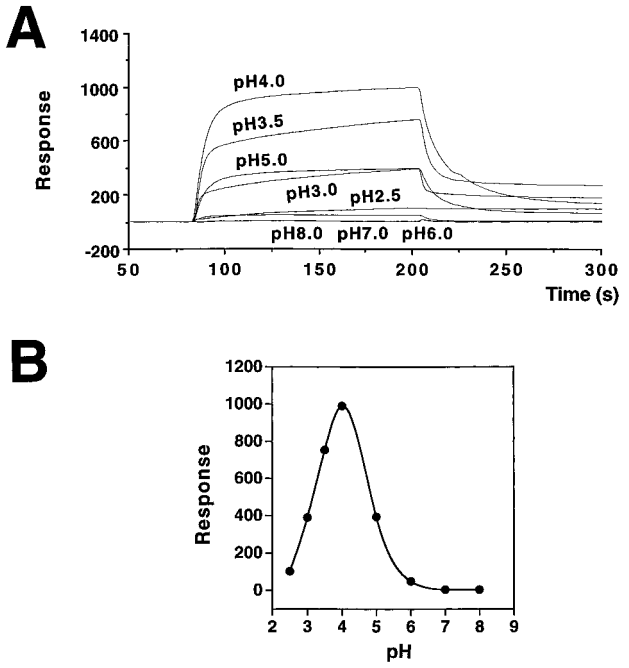

FIGURE 3: pH dependence of Bcl-X_L interactions with Bcl-2. In panel A, representative sensorgrams are presented for Bcl-X_L (soluble phase) binding to immobilized Bcl-2 at various pHs as indicated (2.5−8.0). The Bcl-2 containing chip (∼5000 RU) was equilibrated with various interaction buffers, all containing 150 mM NaCl and 3.4 mM EDTA, with 50 mM of either Tris [pH 8.0], sodium phosphate (pH 6.0, 7.0), sodium acetate (pH 3.0, 3.5, 4.0, 5.0), or Gly-HCl (pH 2.5). Bcl-X_L (∼0.4 uM) was injected at 10 μL/min and the binding recorded. After reaching steady state, flow over the chip was continued without Bcl-X_L. In panel B, the maximum RU obtained for binding of Bcl-X_L to the Bcl-2 chip at each pH was plotted, arbitarily normalized relative to the results obtained for pH 8.0.

X_L was observed, with rapid initial binding, which then gradually slowed until a plateau or near plateau steady-state equilibrium was reached. Comparisons with measurements performed at pH 4.0 revealed that the association-phase kinetics for these binding events were not substantially different from those obtained at pH 7.4. In all cases, however, the dissociation rates appeared to be markedly slower at pH 4.0. The binding of Bcl-X_L to Bid-containing chips was the most stable of the protein−protein interactions tested, exhibiting a very slow rate of dissociation at pH 4.0 (Figure 4).

To directly compare the relative dissociation rates at pH 4.0 with 7.4, Bcl-X_L was flowed over either a Bid or a Bcl-2 chip at pH 4.0, and binding was allowed to proceed until equilibrium was reached, then the mobile phase was switched to either pH 4.0 or 7.4 without Bcl-X_L protein. As shown in Figure 5, dissociation of Bcl-X_L from either immobilized Bcl-2 or Bid was considerably slower at pH 4.0 compared to pH 7.4. Though the rapid rate of dissociation at pH 7.4 precluded accurate determination, the estimated k_d values were roughly 15-fold lower for Bcl-2/Bcl-X_L (0.05 μM/s versus 0.74 μM/s) and ∼60-fold lower for Bcl-X_L/Bid (0.009 μM/s versus 0.55 μM/s).

Table 1 contrasts the apparent equilibrium dissociation constants for Bcl-X_L binding to Bcl-2, Bax, Bid, and Bcl-X_L at pH 4.0 and 7.4. The apparent K_D for Bcl-X_L dimerization with all proteins tested was ∼14 to ∼63 times lower at pH 4.0 compared to pH 7.4, indicating a substantially higher affinity interaction at lower pH.

BH3 Domain Dependence of Interactions of Bcl-X_L with Other Bcl-2 Family Proteins. Previous studies have demonstrated that dimerization among Bcl-2 family proteins depends on insertion of the BH3 domain of one partner into a surface hydrophobic pocket on the other (*15*). To determine whether the interactions measured here by SPR at low pH are BH3 dependent, a synthetic peptide representing the BH3 domain of Bax was tested for ability to inhibit binding of Bcl-X_L to immobilized Bid at pH 4.0. Bid was chosen for these experiments because its binding to Bcl-X_L occurred with the highest affinity among the Bcl-2 family proteins tested. As shown in Figure 6, addition of a 16 mer BH3 Bax peptide produced a concentration-dependent inhibition of the interaction of Bcl-X_L with immobilized Bid, with an IC50 of ∼25 μM. Similar results were obtained when the effects of the BH3 domain peptide were tested on interactions of Bcl-X_L with Bcl-2 and Bax (data not presented). A variety of unrelated non-BH3 peptides however had little or no effect (Figure 6 and data not shown).

Size-Exclusion Chromatography Analysis of Bcl-X_L Suggests Induction of a Conformational Change at Low pH. Size-exclusion chromatography was used to compare the state of the Bcl-X_L protein at neutral and low pH, making comparisons with the BH3-only protein Bid. When chromatographed on Superdex 200 at either pH 7.4 or 4.0, Bcl-X_L eluted as a single peak corresponding to monomeric protein (Figure 7A and data not shown). Similar results were obtained with Bid at pH 7.4 and 4.0, which also was present as a monomer. Thus, low pH does not promote oligomerization of Bcl-X_L or Bid.

When nonionic detergent (0.1% Tween 20) was included during chromatographic analysis of Bcl-X_L on Superdex 200 at pH 7.4, some Bcl-X_L eluted at higher molecular weight (Figure 7B), in addition to the monomeric Bcl-X_L seen previously at neutral pH in the absence of detergent. At pH 4.0 in the presence of detergent, the majority of the Bcl-X_L eluted from the column as a larger complex (Figure 7C). In contrast, the Bid protein continued to behave as a monomer when analyzed by gel-sieve chromatography even at low pH and in the presence of detergent. Since the large complexes of Bcl-X_L were not observed when the detergent was absent (not shown), we interpret this pH and detergent-dependent alteration in the chromatographic behavior of Bcl-X_L as evidence either that Bcl-X_L associates with detergent vesicles at pH 4.0 or that the combination of low pH and detergent promotes conformational changes in Bcl-X_L that allow it to oligomerize. The observation that Bid does not exhibit this altered behavior is consistent both with its predicted lack of structural similarity to pore-forming proteins and its reported inability to homodimerize (*5*). Interestingly, it has recently been reported that nonionic detergents can induce dimerization among members of the Bcl-2 family as a post-cell-lysis event (*36*).

BisANS Fluorescence Studies Indicate Exposure of Hydrophobic Regions of Bcl-X_L at Low pH. The fluorochrome BisANS associates with hydrophobic regions on proteins, such that the extent of emissions at 490 nm is an indication of the relative hydrophobicity of a protein (*34*). We therefore compared the BisANS labeling of Bcl-X_L over the pH range of 2.5−8.0. As shown in Figure 8, the relative amount of BisANS association with the Bcl-X_L protein increased at pH <6.0, reaching a maximum at pH 3.0−4.0. Over the same

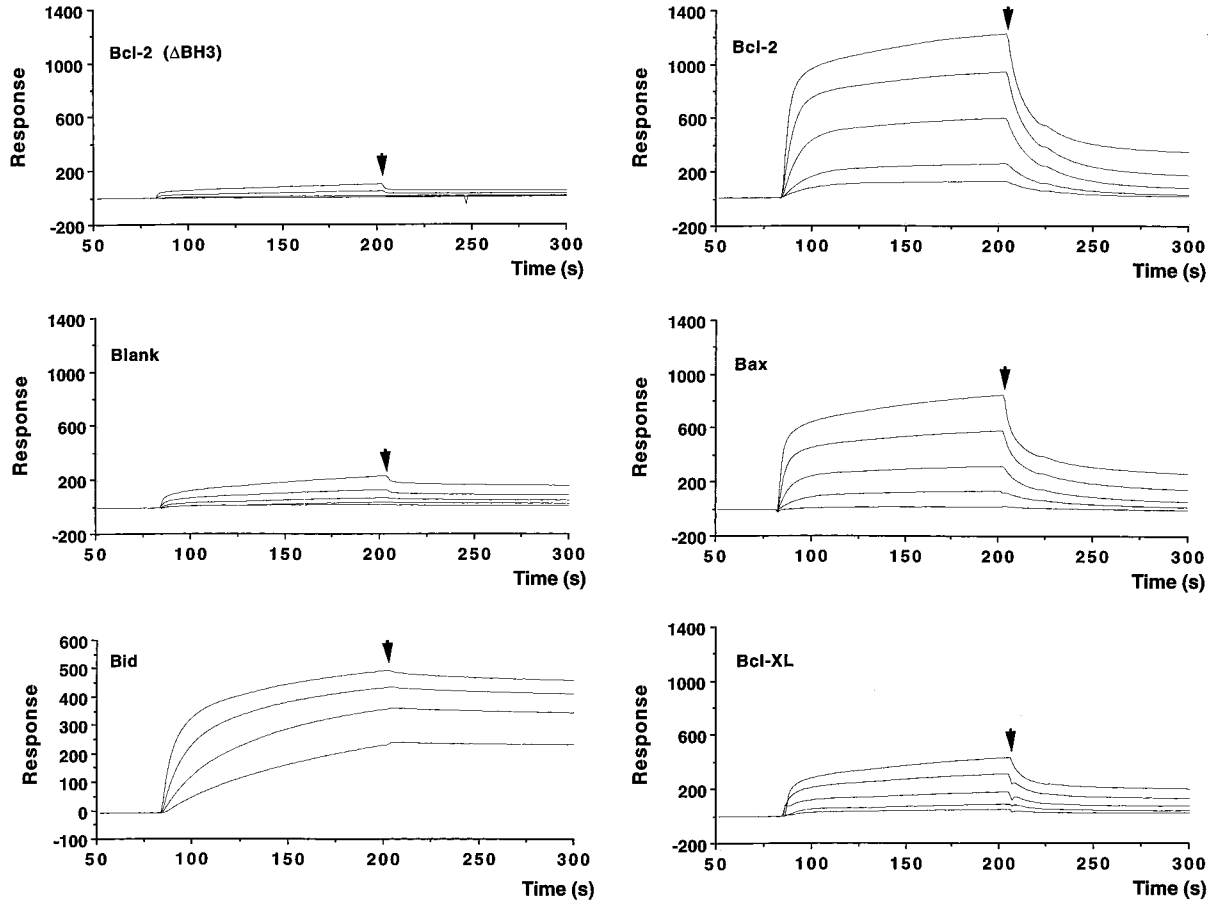

FIGURE 4: Kinetics of Bcl-X_L interactions with other Bcl-2 family proteins at acidic pH. SPR analysis was conducted at pH 4.0, flowing Bcl-X_L at various concentrations over chips containing immobilized Bcl-2, Bax, Bid, Bcl-X_L, or Bcl-2 (ΔBH3) (~5000 RU). Alternatively, the chip was inactivated with ethanolamine to block reactive groups and Bcl-X_L was flowed over the blank chip. Bcl-X_L at ~50−750 nM was injected (20 μL) at a flow rate of 10 μL/min. The binding and dissociation were recorded. The chip was regenerated using 5 μL of 4 M GuHCl containing 50 mM Sodium phosphate (pH 6.8) after each injection.

pH range, the basal fluorescence from BisANS was stable. Thus, acidic pH in the 3.0−4.0 range appears to induce the Bcl-X_L protein to undergo conformational changes which result in exposure of hydrophobic surfaces of this protein.

Circular Dichroism Analysis of Bcl-X_L and Bax Proteins Indicates Retention of Overall Secondary Structure at Low pH. One concern with studies of Bcl-2 family proteins performed at pH 4.0 is whether they become denatured and thus nonspecifically adsorb to each other or expose hydrophobic regions. To address this concern, circular dichroism (CD) analysis was performed for Bcl-X_L and Bax at pH 4.0 and 7.0, using the far-UV region which is sensitive to secondary structure. The far-UV CD spectra for these proteins were nearly superimposable at pH 4.0 and 7.0, indicating retention of their overall α-helical content and secondary structure. Figure 9, for example, shows the far-UV spectra for Bcl-X_L at pH 4.0 and 7.0. Note the retention of the absorption minima at 208 and 222 nm at pH 4.0, which is characteristic of α-helical proteins. These data therefore argue that the secondary structure of this protein is preserved at low pH, implying that acidic pH does not denature Bcl-2 family proteins.

DISCUSSION

The data presented here provide the first kinetic analysis of dimerization among Bcl-2 family proteins. Consistent with previous studies, the protein−protein interactions detected by SPR analysis appear to be dependent on the BH3 domain, based on the observations that: (a) deletion of the BH3 domain from Bcl-2 abolished its interactions with Bcl-X_L and (b) a BH3 peptide abrogated binding in SPR experiments. Interestingly, at acidic pH, the relative affinity of interactions among Bcl-2 family proteins was increased. The basis for this increased affinity was attributable primarily to a markedly reduced dissociation rate. Thus, Bcl-X_L complexes with Bcl-2, Bax, or Bid were considerably more stable at pH 4.0 than at pH 7.0−7.4.

The molecular basis for the increased stability of Bcl-X_L complexes with Bcl-2, Bax, and Bid could have several explanations. First, protonation of specific residues directly involved in binding could increase the stability of these protein complexes, perhaps by reducing electrostatic repulsions or increasing hydrophobicity and thus promoting hydrophobic interactions. Second, low pH could promote or stabilize a conformational change in these proteins which then indirectly affects binding. Third, acidic pH could help to decrease the rigidity of Bcl-X_L and other Bcl-2 family proteins, loosening their α-helical segments from intramolecular interactions with each other and creating more flexibility for dimerization. In this regard, Bcl-X_L and the structurally similar pore-forming domains of the colicins and diphtheria toxin are proposed to assume a molten globule state which allows them the flexibility to transition back and forth from tight compact α-helical bundle structures in

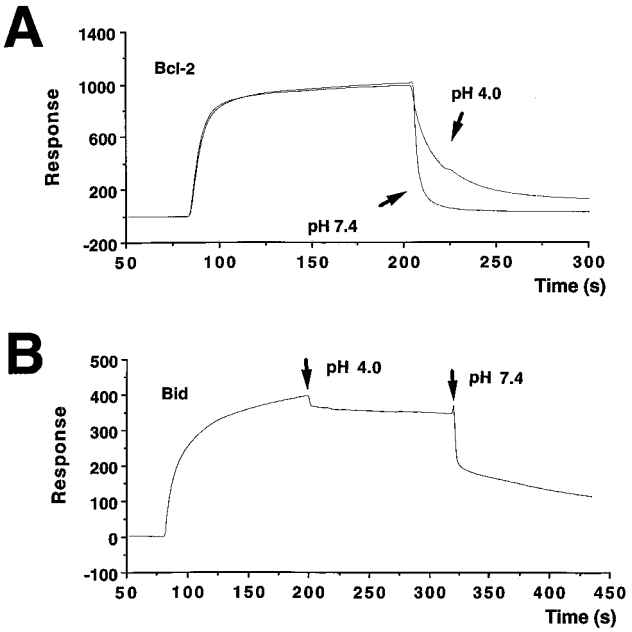

FIGURE 5: Acidic pH decreases rate of dissociation of Bcl-X_L from Bcl-2 family proteins. Bcl-X_L protein (~0.4 uM) in Sodium acetate (pH 4.0), 150 mM NaCl, and 3.4 mM EDTA was flowed across chips containing either immobilized (A) Bcl-2 or (B) Bid protein (~5000 RU) and binding was allow to proceed until steady state was reached. Dissociation was then monitored at pH 4.0 by continuing flow of the same solution or at pH 7.4 by switching to phosphate-buffered (pH 7.4) saline/EDTA solution. In panel B, dissociation was initiated at pH 4.0, and then the buffer was switched to pH 7.4 at the indicated time (arrow).

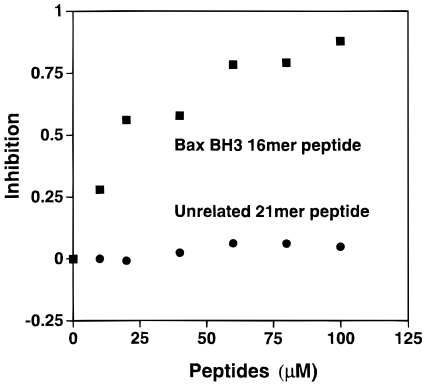

FIGURE 6: BH3 domain dependence of Bcl-X_L dimerization with other Bcl-2 family proteins. Bcl-X_L (~0.3 μM) alone or in combination with various concentrations of either 16 mer Bax BH3 peptide or unrelated 21 mer was flowed over a Bid-containing chip (~1500 RU) at pH 4.0. Injections were performed using 20 μL of Bcl-X_L solution at 10 μL/min, with regeneration in 4 M GuHCl (pH 6.8) between injections.

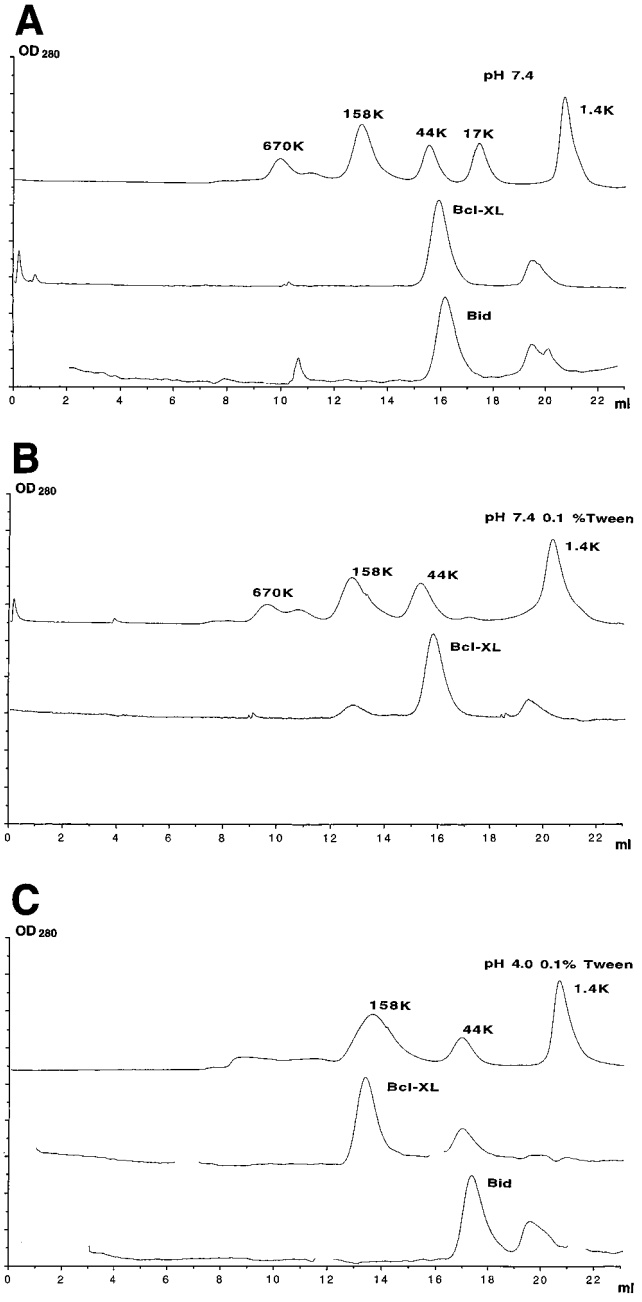

FIGURE 7: Analysis of Bcl-X_L and Bid at acidic and neutral pH by gel-filtration chromatography. Bcl-X_L or Bid protein (25 μg in 50 μL) was applied to a Superdex 200 (10/30) column previously equilibrated with 10 mM HEPES (pH 7.4), 150 mM NaCl, and 3.4 mM EDTA without (A) or with 0.1% (v/v) Tween 20 (B). Alternatively, chromatography was performed in 50 mM Sodium acetate [pH 4.0], 150 mM NaCl, and 3.4 mM EDTA with 0.1% Tween 20 (C). The locations of the protein standards are indicated at the top of each panel.

aqueous environments to membrane inserted molecules with much looser packing of their α-helices (*37*, *38*). Consistent with the requirement of the molten globule state, our CD analysis suggested no changes in overall α-helical content of Bcl-X_L when compared at pH 4.0 and 7.0−7.4, implying a preservation of secondary structure.

It should be emphasized that the affinities (K_D) and kinetic constants (k_a, k_d) obtained here by SPR are merely apparent values (*28*). For the purpose of these studies, the importance of the determined K_D and rate constants permits comparisons of the *relative* changes in K_D and in association and dissociation rates at acidic versus neutral pH. For example, the relative affinity of Bcl-X_L/Bid heterodimerization at pH 4.0 compared to pH 7.0 was estimated by SPR to be ~63-fold greater (ΔK_D), whereas Bcl-X_L/Bcl-X_L homodimerization was only ~14-fold greater at pH 4.0. Hence, acidic pH has a greater impact on stabilizing Bcl-X_L/Bid complexes than Bcl-X_L/Bcl-X_L complexes. Consistent with these data, Bcl-X_L migrated predominantly as a monomer in gel-sieve chromatography experiments even at pH 4.0.

Several lines of evidence support the idea that acidic pH either induces a specific conformational change in Bcl-2 family proteins or loosens the packing of their α-helices,

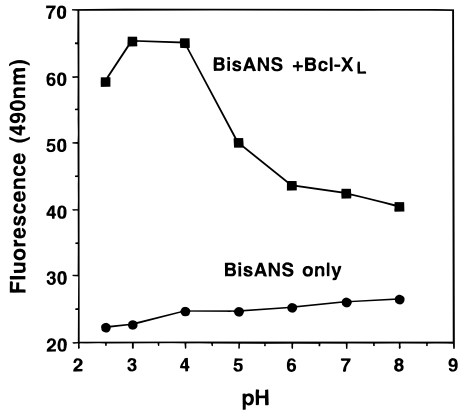

FIGURE 8: pH effects on bisANS binding to Bcl-X_L. BisANS (4,4′-dianilino-1,1′-binaphthyl-5,5′-disulfonic acid) (~10 μM) was mixed with ~0.2 μM Bcl-XL at various pH conditions (50 mM buffer, Tris-HCl, pH 8.0, Sodium phosphate, pH 7.0, pH 6.0, Sodium acetate, pH 5.0, pH 4.0, pH 3.0, Gly-HCl, pH 2.5) in 150 mM NaCl, and 3.4 mM EDTA. Samples were incubated at 25 °C for 0.5 h, and excited at 294 nm. Emission at 490 nm were recorded and plotted against pH.

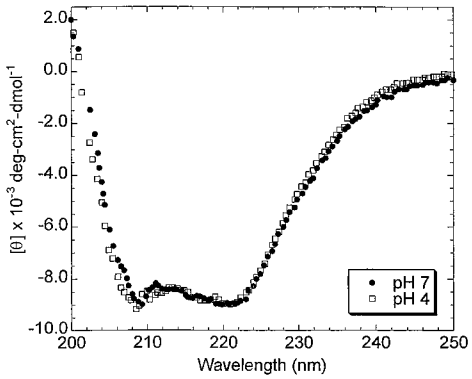

FIGURE 9: Circular dichroism (CD) analysis of Bcl-X_L at pH 4.0 and 7.0. The secondary structure at pH 4.0 and 7.0 was monitored by scanning from 200 to 250 nm in a 1 mm path length cell. Bcl-X_L was dissolved in 20 mM DMG and 100 mM NaCl, pH 4.0 (squares) or 7.0 (circles). Each spectrum represents the average of five scans corrected for background intensity by subtraction of the buffer blank.

thus providing greater flexibility for dimerization. First, recent structural analysis by NMR of BH3 peptides bound to the hydrophobic surface pocket of Bcl-X_L implies a need for a conformation among Bcl-2 family proteins in which the amphipathic α-helix that comprises the BH3 domain is rotated outward to expose its hydrophobic surface for interactions with the hydrophobic pocket on Bcl-X_L (*15*). Second, studies of ion-channel formation by Bcl-X_L, Bcl-2, and Bax using synthetic liposomes have shown that low pH (~4.0) markedly enhances channel activity and indeed is required for converting the bulk of the molecules into a state that is competent to form ion channels in vitro (*20, 21, 23*). By analogy to structurally similar pore-forming domains of bacterial toxins (*39*), channel formation by Bcl-2 and Bcl-X_L is predicted to require insertion of the hydrophobic α5 and α6 helical hairpin perpendicularly into the lipid bilayer, with the surrounding amphipathic α-helices (which include BH3) folding away from the core hydrophobic helices analogous to the opening of an umbrella. This membrane-insertion competent conformation of the protein ("open conformation") is presumably favored by low pH and would presumably extricate the BH3 domain from its normal docking site against the core hydrophobic α5 and α6 helices, freeing it for dimerization with other Bcl-2 molecules that retain the compact α-helical bundle structure ("closed conformation") that creates a hydrophobic pocket on the surface of the protein. Third, comparisons of Bcl-X_L by gel chromatography at neutral and acidic pH in the presence of detergents suggest that low pH induces a conformation which promotes Bcl-X_L association with detergent vesicles or induces its oligomerization. Fourth, labeling with BisANS suggests greater exposure of hydrophobic regions within Bcl-X_L at low pH. Fifth, CD studies indicate no overall change in secondary structure of Bcl-X_L at pH 4.0 compared to pH 7.0, implying that the α-helical regions of the protein remain intact and that a denaturation of the protein cannot account for increased exposure of hydrophobic regions at acidic pH.

The relevance of the enhanced affinity of dimerization seen at acidic pH to the pore-forming activity of Bcl-2 family proteins remains to be determined. When applied to liposomes, the ability of Bcl-2, Bcl-X_L, and Bax to form ion-conducting channels is greatly enhanced by low pH, with optimal pH typically ~4.0 (*20*−*22*). Because dimerization among Bcl-2 family proteins is preserved and even enhanced at low pH, it could be speculated that homodimerization facilitates the process of membrane insertion. In contrast, certain heterodimerization events might impair integration and channel formation at low pH, such as those involving pore-forming Bcl-X_L-like proteins with BH3-only proteins such as Bid. Alternatively, if not altering the actual process of insertion, homodimerization might enhance channel formation by placing two protein molecules in contact with each other once in the membrane. This is because Bcl-X_L contains only two α-helices which are sufficiently long to span the planar bilayer (α5 and α6) (*14*), and yet a minimum of four α-helices integrated into the membrane has been shown to be required for creating ion-conducting channels in vitro (*24, 25*). This implies that at least two Bcl-X_L, Bcl-2, or Bax molecules must collaborate in membranes to create a channel.

Though acidic pH can evidently alter the binding behavior and presumably the conformation of Bcl-X_L and other Bcl-2 family proteins in vitro, the question is what controls these events in vivo? Acidic pH of ~4.0 does not occur within the cytosol of cells, probably not even under pathological situations. However, it may be relevant that many Bcl-2 family proteins are anchored in the outer membrane of mitochondria (*40*). A proton gradient exists across the inner membrane of these organelles, creating an acidic pH environment of ~6.0−6.5 in the space between the inner and outer mitochondria membranes (*41*). The influence of this pH gradient on Bcl-2 family proteins might be most pronounced at the contact sites where the inner and outer membranes abut and where various transport phenomena occur. Interestingly, previous immuno-electron microscopy studies have localized Bcl-2 predominantly to these contact sites (*42*). Thus, while insufficient by itself, the lower pH environment of the mitochondrial intermembrane space may facilitate dimerization among Bcl-2 family proteins.

In addition to local pH effects, interactions with other proteins may also influence dimerization among Bcl-2 family proteins in vivo. In this regard, evidence that Bcl-2 may interact with components of the Hsp70-family of chaperones has been obtained. Specifically, a Hsp70/Hsc70-binding

protein BAG-1 (also known as HAP-1 and RAP46) has been identified which can interact with Bcl-2 and enhance its anti-apoptotic function (*43*−*45*). The implication of these findings is that Bcl-2 can be recognized by Hsc70/BAG-1 complexes, thus providing a potential mechanism for modulating the conformation of Bcl-2 in cells. Other protein interactions with Bcl-2 could also conceivably alter its conformation in ways that might impact on dimerization with Bcl-2 family proteins (reviewed in refs *3* and *35*). Regardless of the in vivo mechanisms involved, the data reported here showing that acidic pH stabilizes dimerization among Bcl-2 family proteins provide insights into the biophysical properties of these proteins which may be relevant to their mechanisms of ion-channel formation.

ACKNOWLEDGMENT

We thank H. Gallant for manuscript preparation, K. Ely, J. Stewart, J. Smith, and D. Hu for helpful discussions.

REFERENCES

1. Reed, J. C. (1994) *J. Cell Biol. 124*, 1−6.
2. Yang, E., and Korsmeyer, S. J. (1996) *Blood 88*, 386-401.
3. Kroemer, G. (1997) *Nat. Med. 3*, 614−20.
4. Boyd, J. M., Gallo, G. J., Elangovan, B., Houghton, A. B., Malstrom, S., Avery, B. J., Ebb, R. G., Subramanian, T., Chittenden, T., Lutz, R. J., and Chinnadurai, G. (1995) *Oncogene 11*, 1921−1928.
5. Wang, K., Yin, W.-M., Chao, D. T., Milliman, C. L., and Korsmeyer, S. J. (1996) *Genes Dev. 10*, 2859−2869.
6. O'Connor, L., Strasser, A., O'Reilly, L. A., Adams, J. M., Cory, S., and Huang, D. C. S. (1997) *EMBO J.* (In press).
7. Yin, X. M., Oltvai, Z. N., and Korsmeyer, S. J. (1994) *Nature 369*, 321−333.
8. Hanada, M., Aimé-Sempé, C., Sato, T., and Reed, J. C. (1995) *J. Biol. Chem. 270*, 11962−11968.
9. Bodrug, S. E., Aimé-Sempé, C., Sato, T., Krajewski, S., Hanada, M., and Reed, J. C. (1995) *Cell Death Differ. 2*, 173−182.
10. Zha, H., Aime-Sempe, C., Sato, T., and Reed, J. C. (1996) *J. Biol. Chem. 271*, 7440−7444.
11. Chittenden, T., Flemington, C., Houghton, A. B., Ebb, R. G., Gallo, G. J., Elangovan, B., Chinnadurai, G., and Lutz, R. J. (1995) *EMBO J. 14*, 5589−5596.
12. Sedlak, T. W., Oltvai, Z. N., Yang, E., Wang, K., Boise, L. H., Thompson, C. B., and Korsmeyer, S. J. (1995) *Proc. Natl. Acad. Sci. U.S.A. 92*, 7834−7838.
13. Inohara, N., Ding, L., Chen, S., and Nunez, G. (1997) *EMBO J. 16*, 1686−1694.
14. Muchmore, S. W., Sattler, M., Liang, H., Meadows, R. P., Harlan, J. E., Yoon, H. S., Nettesheim, D., Changs, B. S., Thompson, C. B., Wong, S., Ng, S., and Fesik, S. W. (1996) *Nature 381*, 335−341.
15. Sattler, M., Liang, H., Nettesheim, D., Meadows, R. P., Harlan, J. E., Eberstadt, M., Yoon, H. S., Shuker, S. B., Chang, B. S., Minn, A. J., Thompson, C. B., and Fesik, S. W. (1997) *Science 275*, 983−986.
16. Zha, H., Aime-Sempe, C., Sato, T., and Reed, J. C. (1996) *J. Biol. Chem. 271*, 7440−7444.
17. Zha, H., Fisk, H. A., Yaffe, M. P., Mahajan, N., Herman, B., and Reed, J. C. (1996) *Mol. Cell. Biol. 16*, 6494−6508.
18. Diaz, J.-L., Oltersdorf, T., Horne, W., McConnell, M., Wilson, G., Weeks, S., Garcia, T., and Fritz, L. C. (1997) *J. Biol. Chem. 272*, 11350−11355.
19. Schendel, S., Montal, M., and Reed, J. C. (1997) *Cell Death Differ.* (In press).
20. Minn, A. J., Velez, P., Schendel, S. L., Liang, H., Muchmore, S. W., Fesik, S. W., Fill, M., and Thompson, C. B. (1997) *Nature 385*, 353−357.
21. Schendel, S. L., Xie, Z., Montal, M. O., Matsuyama, S., Montal, M., and Reed, J. C. (1997) *Proc. Natl. Acad. Sci. U.S.A. 94*, 5113−5118.
22. Antonsson, B., Conti, F., Ciavatta, A., Montessuit, S., Lewis, S., Martinou, I., Bernasconi, L., Bernard, A., Mermod, J.-J., Mazzei, G., Maundrell, K., Gambale, F., Sadoul, R., and Martinou, J.-C. (1997) *Science 277*, 370−372.
23. Schlesinger, P., Gross, A., Yin, X.-M., Yamamoto, K., Saito, M., Waksman, G., and Korsmeyer, S. (1997) *Proc. Natl. Acad. Sci. U.S.A. 94*, 11357−11362.
24. Oblatt-Montal, M., Buhler, L. K., Iwamoto, T., Tomich, J. M., and Montal, M. (1993) *J Biol Chem 268*, 14601−14607.
25. Reddy, L. G., Iwamoto, T., Tomich, J. M., and Montal, M. (1993) *J. Biol. Chem. 268*, 14608−14615.
26. Raghavan, M., and Bjorkman, P. J. (1995) *Curr. Biol. 3*, 331−333.
27. Fisher, R. J., and Fivash, M. (1994) *Curr. Opin. Biotech. 5*, 389−395.
28. Schuck, P. (1997) in *Annu. Rev. Biophys. Struct.* (Stroud, R. M., Ed.) pp 541−566, Annual Reviews Inc., Palo Alto, CA.
29. Fägerstam, L. G., Frostell-Karlsson, Å., Karlsson, R., Persson, B., and Rönnberg, I. (1992) *J. Chromatogr. A 597*, 397−410.
30. Chaiken, I., Rosé, S., and Karlsson, R. (1992) *Anal. Biochem. 201*, 197−210.
31. Zha, H., and Reed, J. C. (1997) *J. Biol. Chem. 272*, 31482−31488.
32. Wang, H.-G., Takayama, S., Rapp, U. R., and Reed, J. C. (1996) *Proc. Natl. Acad. Sci. U.S.A. 93*, 7063−7068.
33. Wang, H. G., Rapp, U. R., and Reed, J. C. (1996) *Cell 87*, 629−638.
34. Rosen, C. G., and Weber, G. (1969) *Biochemistry 8*, 3915−3920.
35. Reed, J. C. (1997) *Nature 387*, 773−776.
36. Hsu, Y. T., and Youle, R. J. (1997) *J. Biol. Chem. 272*, 13829−13834.
37. van der Goot, F. G., Gonzalez-Manas, J. M., Lakey, J. H., and Pattus, F. (1991) *Nature 354*, 408−410.
38. Ramsay, G., Montgomery, D., Berger, D., and Freire, E. (1989) *Biochemistry 28*, 529−533.
39. Cramer, W. A., Heymann, J. B., Schendel, S. L., Deriy, B. N., Cohen, F. S., Elkins, P. A., and Stauffacher, C. V. (1995) *Annu. Rev. Biophys. Biomol. Struct. 24*, 611−641.
40. Krajewski, S., Tanaka, S., Takayama, S., Schibler, M. J., Fenton, W., and Reed, J. C. (1993) *Cancer Res 53*, 4701−4714.
41. Alberts, B., Bray, D., Lewis, J., Raff, M., Roberts, K., and Watson, J. D. (1994) in *Molecular Biology of the Cell* (Robertson, M., Ed.) pp 653−720, Garland Publishing, Inc., New York.
42. de Jong, D., Prins, F. A., Mason, D. Y., Reed, J. C., van Ommen, G. B., and Kluin, P. M. (1994) *Cancer Res. 54*, 256−260.
43. Takayama, S., Sato, T., Krajewski, S., Kochel, K., Irie, S., Millan, J. A., and Reed, J. C. (1995) *Cell 80*, 279−284.
44. Takayama, S., Bimston, D. N., Matsuzawa, S., Freeman, B. C., Aime-Sempe, C., Xie, Z., Morimoto, R. J., and Reed, J. C. (1997) *EMBO J. 16*, 4887−4896.
45. Zeiner, M., Gebauer, M., and Gehring, U. (1997) *EMBO J. 16*, 5483−5490.

BI973052I